

Supporting Information “Quantum logic gates based on DNAtronics, RNAtronics and Proteintronics”

Sheh-Yi Sheu^{1,2}, Hua-Yi Hsu¹, and Dah-Yen Yang³

¹Department of Life Sciences and Institute of Genome Sciences, National Yang Ming Chiao Tung University, Taipei 112, Taiwan

²Institute of Biomedical Informatics, National Yang Ming Chiao Tung University, Taipei 112, Taiwan

³Institute of Atomic and Molecular Sciences, Academia Sinica, Taipei, Taiwan

March 1, 2021

Abstract

This Supporting Information includes the extended description of the superposition state of the asymmetric double-well system in vacuum system and in solution, truth tables for the residue pairs and their corresponding quantum logic gates, and figures for the double well potential energy surfaces and transmission spectra of the residue pairs.

Corresponding Authors

Email: sysheu@ym.edu.tw and dyyang@pub.iams.sinica.edu.tw

Appendix

A. Superposition state of an asymmetric double-well system in vacuum

Let us consider an asymmetric double-well system with two local minimum states $|0\rangle$ and $|1\rangle$ for the wells 0 and 1, respectively, in vacuum (Figure S2 (a)). For an unperturbed system, we define the Hamiltonian operator as H_0 . The eigenstates are $|0\rangle$ and $|1\rangle$ with respect to the atomic orbitals and their eigenvalues are E_0 and E_1 . The approximate solution $\psi = c_0|0\rangle + c_1|1\rangle$, corresponding to the molecular orbital, of the double-well system satisfies the Schrödinger equation

$$H\psi = E\psi \tag{A1}$$

where $H = H_0 + H_1$, H_1 is the external perturbed Hamiltonian operator, and E is the

eigenvalue. In order to solve the mixing coefficients c_0 and c_1 , we multiply both sides of Eq.(1) with $|0\rangle$ and $|1\rangle$, and integrate the coordinate from $-\infty$ to ∞ . Then, we can obtain

$$\begin{aligned} H_{00} c_0 + H_{01} c_1 &= E c_0 \\ H_{10} c_0 + H_{11} c_1 &= E c_1 \end{aligned} \quad (\text{A2})$$

where $H_{ij} = \int \langle i|H|j\rangle dx$, (i and $j = 0, 1$), $\int \langle 0|0\rangle dx = \int \langle 1|1\rangle dx = 1$ and $\int \langle 0|1\rangle dx \approx 0$. Equations (A2) are a set of the secular equation with two variables (c_0 and c_1). The coefficients are $H_{00} = E_0$, $E_{11} = E_1$, and $H_{01} = H_{10} = -V (V > 0)$.

Based on an asymmetric double-well system with two distinct E_0 and E_1 (Figures S2(a)), Eq.(A2) can be rewritten as

$$\begin{bmatrix} E_0 - E & -V \\ -V & E_1 - E \end{bmatrix} \begin{bmatrix} c_0 \\ c_1 \end{bmatrix} = 0$$

Typically, $(c_0, c_1) \neq (0, 0)$, the determinant of the 2×2 matrix is vanished, and the eigenenergies are $E \equiv E_{\pm} = \frac{E_0+E_1}{2} \pm \sqrt{\left(\frac{E_0-E_1}{2}\right)^2 + V^2}$, where E_- and E_+ are the energies for the ground state and the excited state, respectively (Figure S2(b)).

The ratios of population at the ground state and at the excited state are

$(\frac{c_1}{c_0})_{\text{ground}} = \frac{E_{av} + \sqrt{\Delta^2 + V^2}}{V}$ and $(\frac{c_1}{c_0})_{\text{excited}} = \frac{E_{av} - \sqrt{\Delta^2 + V^2}}{V}$, where $\Delta = \frac{E_0 - E_1}{2}$ and $E_{av} = \frac{E_0 + E_1}{2}$. Then, the excited state and the ground state are $\psi_+ = \cos(\frac{\theta}{2}) e^{-i\frac{\phi}{2}} |0\rangle + \sin(\frac{\theta}{2}) e^{i\frac{\phi}{2}} |1\rangle$ and $\psi_- = -\sin(\frac{\theta}{2}) e^{-i\frac{\phi}{2}} |0\rangle + \cos(\frac{\theta}{2}) e^{i\frac{\phi}{2}} |1\rangle$, respectively, where $\tan \theta = |V|/\Delta$ and $V = |V|e^{i\phi}$.

Furthermore, let us apply this double-well system to the H-bond, i.e. N-H ... O, in vacuum, and adopt the atomic orbitals from N and O atoms as $|0\rangle = \psi_N$ and $|1\rangle = \psi_O$. Initially, the proton is located at the $|0\rangle$ state close to the N-atom. We here define the initial state at $t = 0$ as $\psi(0) = |0\rangle = e^{i\frac{\phi}{2}} [\cos(\frac{\theta}{2}) \psi_+ - \sin(\frac{\theta}{2}) \psi_-]$. The time evolution of the state follows

$$\begin{aligned} \psi(t) &= U(t, 0) \psi(0) = e^{-i\frac{Ht}{\hbar}} \psi(0) \\ &= e^{i\frac{\phi}{2}} [\cos(\frac{\theta}{2}) e^{-i\frac{E_+ t}{\hbar}} \psi_+ - \sin(\frac{\theta}{2}) e^{-i\frac{E_- t}{\hbar}} \psi_-] \\ &= c_0 |0\rangle + c_1 |1\rangle \end{aligned} \quad (\text{A3})$$

where

$$c_0 = \left(\cos^2(\frac{\theta}{2}) e^{-i\frac{E_+ t}{\hbar}} + \sin^2(\frac{\theta}{2}) e^{-i\frac{E_- t}{\hbar}} \right) \quad (\text{A4})$$

and

$$c_1 = \frac{1}{2} \cos(\theta) e^{i\phi} (e^{-i\frac{E_+ t}{\hbar}} - e^{-i\frac{E_- t}{\hbar}}) \quad (\text{A5})$$

are complex amplitudes and satisfy the relationship $|c_0|^2 + |c_1|^2 = 1$. This proves the superposition state of qubit.

B. Superposition state of an asymmetric double-well in solution: spin-boson model

Let us consider a simplified double-well system embedded in solution by using the spin-boson model in which the spin part denotes the H-bond system and the bosonic part mimics the solvent degrees of freedom. The total Hamiltonian operator of this model is then given by

$$\begin{aligned} H &= H_S + H_B + H_{SB} \\ &= -\frac{1}{2}\hbar\Delta_0 \sigma_x + \frac{1}{2}\epsilon \sigma_z + \sum_{\gamma} \hbar\omega_{\gamma} \hat{b}_{\gamma}^{\dagger} \hat{b}_{\gamma} + \sigma_z \sum_{\gamma} c_{\gamma} (\hat{b}_{\gamma} + \hat{b}_{\gamma}^{\dagger}) \end{aligned}$$

and

$$\begin{aligned} H_0 &= H_S + H_B \\ H_S &= -\frac{1}{2} \hbar\Delta_0 \sigma_x + \frac{1}{2} \epsilon \sigma_z \\ H_B &= \sum_{\gamma} \hbar\omega_{\gamma} \hat{b}_{\gamma}^{\dagger} \hat{b}_{\gamma} \\ H_{SB} &= \sigma_z \sum_{\gamma} c_{\gamma} (\hat{b}_{\gamma} + \hat{b}_{\gamma}^{\dagger}) \end{aligned}$$

where the sum is based on the bosonic modes. Here, the parameter ϵ denotes the energy difference between the ground-state energies of the states localized in the two wells without tunneling, and Δ_0 indicates the matrix for tunneling between the two wells (Figure S2 (c)). The σ_x, σ_y and σ_z are Pauli operators while $\hat{b}_{\gamma}^{\dagger}$ and \hat{b}_{γ} are the creation and annihilation operators acting on the γ th bosonic mode of the heat bath and they obey the relationship $[\hat{b}_{\gamma}, \hat{b}_{\delta}^{\dagger}] = \delta_{\gamma\delta}$. The c_{γ} is the coupling strength between the γ th bosonic mode and the wells. The dynamics of σ_z depends on the ratio of $\hbar\Delta_0/\epsilon$. The eigenvalue of H_S is $E_{\pm} = \pm\frac{1}{2}\sqrt{\epsilon^2 + (\hbar\Delta_0)^2}$. Here, $|1\rangle \prod_{\gamma} |g_{\gamma 1}\rangle$ and $|0\rangle \prod_{\gamma} |g_{\gamma 0}\rangle$ denote the ground states in the separated right and left isolated local minimum, respectively. Note that $\prod_{\gamma} |g_{\gamma i}\rangle$, $i = 0$ and 1 , indicates the ground bosonic states in the well 0 and 1. To estimate the degree of population for each atomic eigenfunction $|0\rangle$ and $|1\rangle$ in the molecular eigenfunction $\psi = e|0\rangle + f|1\rangle$, we adopt the ratio $(\frac{f}{e})$, which satisfies the population in the ground state and the excited state as $(\frac{f}{e})_{\text{ground}} = \frac{\sqrt{\epsilon^2 + (\hbar\Delta_0)^2}}{\hbar\Delta_0}$ and $(\frac{f}{e})_{\text{excited}} = -\frac{\sqrt{\epsilon^2 + (\hbar\Delta_0)^2}}{\hbar\Delta_0}$. Then, the excited state is $\psi_+ = \cos(\frac{\theta}{2}) e^{-i\frac{\phi}{2}} |0\rangle \prod_{\gamma} |g_{\gamma 0}\rangle + \sin(\frac{\theta}{2}) e^{i\frac{\phi}{2}} |1\rangle \prod_{\gamma} |g_{\gamma 1}\rangle$ and the ground state is $\psi_- = -\sin(\frac{\theta}{2}) e^{-i\frac{\phi}{2}} |0\rangle \prod_{\gamma} |g_{\gamma 0}\rangle + \cos(\frac{\theta}{2}) e^{i\frac{\phi}{2}} |1\rangle \prod_{\gamma} |g_{\gamma 1}\rangle$, where $\tan \theta = \hbar\Delta_0/\epsilon$ and $\hbar\Delta_0 = |\hbar\Delta_0| e^{i\phi}$

or $\phi = 0$. By applying the spin system to the H-bond N-H...O in solution, the atomic orbitals of the N and O atoms are denoted as $|0\rangle = \psi_N$ and $|1\rangle = \psi_O$. Initially, the proton is located close to the N-atom. We here define the initial state as $\Psi_S(0) = |0\rangle \prod_\gamma |g_{\gamma 0}\rangle = [\cos(\frac{\theta}{2}) \psi_+ - \sin(\frac{\theta}{2}) \psi_-]$ at $t = 0$ and solve the Schrodinger equation of the time evolution of state $\Psi_S(t) = U_0(t, 0) U_I(t, 0) \Psi_S(0)$, where ‘S’ means Schrodinger picture and ‘I’ indicates the interaction picture. By using the exponential of Pauli identity $\vec{\sigma} = (\sigma_x, \sigma_y, \sigma_z)$ and $\exp(i \theta \vec{v} \cdot \vec{\sigma}) = \cos(\theta) \sigma_0 + i \sin(\theta) \vec{v} \cdot \vec{\sigma}$, where σ_0 = identity 2×2 matrix, we obtain

$$\begin{aligned} U_I(t, 0) &= \exp_+[-\frac{i}{\hbar} \int_0^t d\tau V_I(\tau)] \\ &= \cos(\kappa) \sigma_0 + i \sin(\kappa) (\frac{A(t)}{\kappa} \sigma_x + \frac{B(t)}{\kappa} \sigma_y + \frac{C(t)}{\kappa} \sigma_z) \\ &= \text{evolution operator in the interaction picture} \end{aligned}$$

and

$$\begin{aligned} U_0(t, 0) &= \exp_+[\frac{i}{\hbar} \int_0^t d\tau H_0(\tau)] \\ &= e^{\frac{i}{\hbar} t \sum_\gamma \hbar \omega_\gamma \hat{b}_\gamma^\dagger \hat{b}_\gamma} [\cos(\lambda t) \sigma_0 + i \sin(\lambda t) (-\frac{\Delta_0}{2\lambda} \sigma_x + \frac{\epsilon}{2\lambda} \sigma_z)] \end{aligned}$$

where $\lambda = \frac{1}{2} \sqrt{\Delta_0^2 + (\frac{\epsilon}{\hbar})^2}$. Then, we have the superposition state

$$\Psi_S(t) = c_0 |0\rangle + c_1 |1\rangle \quad (\text{A6})$$

where $|0\rangle = \begin{bmatrix} 0 \\ 1 \end{bmatrix}$ and $|1\rangle = \begin{bmatrix} 1 \\ 0 \end{bmatrix}$, and

$$\begin{aligned} c_0 &= e^{i t \sum_\gamma \omega_\gamma \hat{b}_\gamma^\dagger \hat{b}_\gamma} \{ \cos(\lambda t) (\cos \kappa - i \sin \kappa \frac{C(t)}{\kappa}) \\ &\quad - i \sin(\lambda t) [\frac{\epsilon}{2\lambda \hbar} (\cos \kappa - i \sin \kappa \frac{C(t)}{\kappa}) \\ &\quad + \frac{\Delta_0}{2\lambda} \sin \kappa (\frac{B(t)}{\kappa} + i \frac{A(t)}{\kappa})] \} \prod_\gamma |g_{\gamma 0}\rangle \end{aligned} \quad (\text{A7})$$

$$\begin{aligned} c_1 &= e^{i t \sum_\gamma \omega_\gamma \hat{b}_\gamma^\dagger \hat{b}_\gamma} \{ \cos(\lambda t) \sin \kappa (\frac{B(t)}{\kappa} + i \frac{A(t)}{\kappa}) \\ &\quad + i \sin(\lambda t) [(-\frac{\Delta_0}{2\lambda} (\cos \kappa - i \sin \kappa \frac{C(t)}{\kappa})) \\ &\quad + \frac{\epsilon}{2\lambda \hbar} \sin \kappa (\frac{B(t)}{\kappa} + i \frac{A(t)}{\kappa})] \} \prod_\gamma |g_{\gamma 0}\rangle \end{aligned} \quad (\text{A8})$$

$$\begin{aligned} A(t) &= \frac{1}{2\hbar} \sum_\gamma c_\gamma \{ [\frac{\sin(\omega_\gamma t)}{\omega_\gamma} - \frac{\sin((\omega_\gamma - 2\lambda)t)}{2(\omega_\lambda - 2\lambda)} - \frac{\sin((\omega_\gamma + 2\lambda)t)}{2(\omega_\gamma + 2\lambda)}] (\hat{b}_\gamma^\dagger + \hat{b}_\gamma) \\ &\quad - i [\frac{\cos(\omega_\gamma t) - 1}{\omega_\gamma} + \frac{\cos((\omega_\gamma - 2\lambda)t) - 1}{2(\omega_\lambda - 2\lambda)} + \frac{\cos((\omega_\gamma + 2\lambda)t) - 1}{2(\omega_\gamma + 2\lambda)}] (\hat{b}_\gamma^\dagger - \hat{b}_\gamma) \} \frac{\Delta_0 \epsilon}{2\lambda^2 \hbar} \end{aligned}$$

$$\begin{aligned}
B(t) &= \frac{1}{2\hbar} \Delta_0 \sum_{\gamma} c_{\gamma} \left\{ \left[\frac{\cos((2\lambda - \omega_{\gamma})t) - 1}{2(2\lambda - \omega_{\gamma})} + \frac{\cos((2\lambda + \omega_{\gamma})t) - 1}{2(2\lambda + \omega_{\gamma})} \right] (\hat{b}_{\gamma}^{\dagger} + \hat{b}_{\gamma}) \right. \\
&\quad \left. + i \left[\frac{\sin((2\lambda - \omega_{\gamma})t)}{2(2\lambda - \omega_{\gamma})} + \frac{\sin((2\lambda + \omega_{\gamma})t)}{2(2\lambda + \omega_{\gamma})} \right] (\hat{b}_{\gamma}^{\dagger} - \hat{b}_{\gamma}) \right\} \\
C(t) &= -\frac{1}{2\hbar} \sum_{\gamma} c_{\gamma} \left\{ \left[\frac{\sin(\omega_{\gamma}t)}{\omega_{\gamma}} + \frac{\sin((\omega_{\gamma} - 2\lambda)t)}{2(\omega_{\gamma} - 2\lambda)} + \frac{\sin((\omega_{\gamma} + 2\lambda)t)}{2(\omega_{\gamma} + 2\lambda)} \right] (\hat{b}_{\gamma}^{\dagger} + \hat{b}_{\gamma}) \right. \\
&\quad \left. - i \left[\frac{\cos(\omega_{\gamma}t) - 1}{\omega_{\gamma}} + \frac{\cos((\omega_{\gamma} - 2\lambda)t) - 1}{2(\omega_{\gamma} - 2\lambda)} + \frac{\cos((\omega_{\gamma} + 2\lambda)t) - 1}{2(\omega_{\gamma} + 2\lambda)} \right] (\hat{b}_{\gamma}^{\dagger} - \hat{b}_{\gamma}) \right\} \\
&\quad - \frac{1}{2\hbar} \sum_{\gamma} c_{\gamma} \left\{ \left[\frac{\sin(\omega_{\gamma}t)}{\omega_{\gamma}} - \frac{\sin((\omega_{\gamma} - 2\lambda)t)}{2(\omega_{\gamma} - 2\lambda)} - \frac{\sin((\omega_{\gamma} + 2\lambda)t)}{2(\omega_{\gamma} + 2\lambda)} \right] (\hat{b}_{\gamma}^{\dagger} + \hat{b}_{\gamma}) \right. \\
&\quad \left. - i \left[\frac{\cos(\omega_{\gamma}t) - 1}{\omega_{\gamma}} + \frac{\cos((\omega_{\gamma} - 2\lambda)t) - 1}{2(\omega_{\gamma} - 2\lambda)} + \frac{\cos((\omega_{\gamma} + 2\lambda)t) - 1}{2(\omega_{\gamma} + 2\lambda)} \right] (\hat{b}_{\gamma}^{\dagger} - \hat{b}_{\gamma}) \right\} \frac{(\frac{\epsilon}{\hbar})^2 - \Delta_0^2}{4\lambda^2}
\end{aligned}$$

$$\kappa = \sqrt{A(t)^2 + B(t)^2 + C(t)^2}.$$

In the weak coupling limit by taking $c_{\gamma} \rightarrow 0$, the equations (A7) and (A8) are with respect to the equations (A4) and (A5), while setting $E_{av} = 0$. Here c_0 and c_1 are complex numbers and are temperature dependent. $\Psi_S(t)$ satisfies the superposition state of qubit.

Table S1: Table 1. Structures of the nucleotide base pairs and the definition of the H-bonds and states.

nucleotide	structure	H-bond	state
DNA	AT	$A^{N6-H1\cdots O4}T_{N1\cdots H2\cdots N3}$	DD_{AT}
		$A^{N6-H1\cdots O4}T_{N1\cdots H2\cdots N3}$	DA_{AT}
		$A^{N6\cdots H1-O4}T_{N1\cdots H2\cdots N3}$	AD_{AT}
		$A^{N6\cdots H1-O4}T_{N1\cdots H2\cdots N3}$	AA_{AT}
	DNA-CG	$C^{N4-H1\cdots O6}_{N3\cdots H2\cdots N1}G_{O2\cdots H3\cdots N2}$	DDD_{DNA-CG} DDD_{RNA-CG}
		$C^{N4-H1\cdots O6}_{N3\cdots H2\cdots N1}G_{O2\cdots H3\cdots N2}$	DDA_{DNA-CG} DDA_{RNA-CG}
		$C^{N4-H1\cdots O6}_{N3\cdots H2\cdots N1}G_{O2\cdots H3\cdots N2}$	DAD_{DNA-CG} DAD_{RNA-CG}
		$C^{N4-H1\cdots O6}_{N3\cdots H2\cdots N1}G_{O2\cdots H3\cdots N2}$	DAA_{DNA-CG} DAA_{RNA-CG}
RNA	RNA-CG	$C^{N4\cdots H1-O6}_{N3\cdots H2\cdots N1}G_{O2\cdots H3\cdots N2}$	ADD_{DNA-CG} ADD_{RNA-CG}
		$C^{N4\cdots H1-O6}_{N3\cdots H2\cdots N1}G_{O2\cdots H3\cdots N2}$	ADA_{DNA-CG} ADA_{RNA-CG}
		$C^{N4\cdots H1-O6}_{N3\cdots H2\cdots N1}G_{O2\cdots H3\cdots N2}$	AAD_{DNA-CG} AAD_{RNA-CG}
		$C^{N4\cdots H1-O6}_{N3\cdots H2\cdots N1}G_{O2\cdots H3\cdots N2}$	AAA_{DNA-CG} AAA_{RNA-CG}
	AU	$A^{N6-H1\cdots O4}U_{N1\cdots H2\cdots N3}$	DD_{AU}
		$A^{N6-H1\cdots O4}U_{N1\cdots H2\cdots N3}$	DA_{AU}
		$A^{N6\cdots H1-O4}U_{N1\cdots H2\cdots N3}$	AD_{AU}
		$A^{N6\cdots H1-O4}U_{N1\cdots H2\cdots N3}$	AA_{AU}
GU	GU	$G^{O6\cdots H1-N3}U_{N1\cdots H2\cdots O2}$	DD_{GU}
		$G^{O6\cdots H1-N3}U_{N1\cdots H2\cdots O2}$	DA_{GU}
		$G^{O6\cdots H1-N3}U_{N1\cdots H2\cdots O2}$	AD_{GU}
		$G^{O6\cdots H1-N3}U_{N1\cdots H2\cdots O2}$	AA_{GU}

Table S2: Table 2. Energy barrier for proton transfer in the nucleotide base pairs.

base pair		state		vacuum (kcal mol ⁻¹)		solution (kcal mol ⁻¹)	
		initial	final	ΔG_D	ΔG_A	ΔG_D	ΔG_A
DNA							
A = T	<i>DD_{AT}</i>	<i>AD_{AT}</i>		37.15	1.35	34.47	4.26
		<i>DA_{AT}</i>		18.22	4.26	16.95	7.17
C ≡ G	<i>DDD_{DNA-CG}</i>	<i>ADD_{DNA-CG}</i>		23.91	2.25	26.64	2.47
		<i>DAD_{DNA-CG}</i>		28.03	4.76	20.51	10.17
		<i>DDA_{DNA-CG}</i>		33.42	1.59	29.45	4.76
RNA							
A = U	<i>DD_{AU}</i>	<i>AD_{AU}</i>		36.62	1.72	35.02	4.23
		<i>DA_{AU}</i>		20.14	4.55	17.96	8.41
C ≡ G	<i>DDD_{RNA-CG}</i>	<i>ADD_{RNA-CG}</i>		26.61	1.72	28.44	2.96
		<i>DAD_{RNA-CG}</i>		24.82	4.63	20.43	9.82
		<i>DDA_{RNA-CG}</i>		34.24	1.42	30.22	5.15
G = U	<i>DD_{GU}</i>	<i>AD_{GU}</i>		unstable	unstable	25.68	1.20
		<i>DA_{GU}</i>		24.28	5.36	24.20	5.35

Table S3: Table 3. Truth table of the DNA-CG nucleotide base pair with the phosphate group charge (-1, -1) in the three spin states.

state	spin state								
	singlet			triplet			quintet		
	in		out	α (I_{\uparrow})	β (I_{\downarrow})	I_c	α (I_{\uparrow})	β (I_{\downarrow})	
	x	y	z	z'		z'		z'	
<i>DDA_{DNA-CG}</i>	0	0	0	0	0	0	0	$\neq 0$	1
<i>DDD_{DNA-CG}</i>	0	0	1	1	$\neq 0$	0	0	$\neq 0$	1
<i>DAA_{DNA-CG}</i>	0	1	0	0	0	0	0	0	0
<i>DAD_{DNA-CG}</i>	0	1	1	1	0	0	0	$\neq 0$	1
<i>ADD_{DNA-CG}</i>	1	0	0	0	0	$\neq 0$	1	0	0
<i>ADA_{DNA-CG}</i>	1	0	1	1	0	$\neq 0$	1	$\neq 0$	1
<i>AAD_{DNA-CG}</i>	1	1	0	1	0	$\neq 0$	1	0	0
<i>AAA_{DNA-CG}</i>	1	1	1	0	0	0	0	$\neq 0$	1
logic gate									
Toffoli				none			none		

Table S4: Truth table of the DNA-CG nucleotide base pair in the singlet state.

state	in			Phosphate group charges (left, right)*								
	x	y	z	(0,0)	(0,-1)	(-1,0)	(-1,-1)	(0,-2)	(-2,0)	(-1,-2)	(-2,-1)	(-2,-2)
DDA_{DNA-CG}	0	0	0	0	0	1	0	0	0	0	0	0
DDD_{DNA-CG}	0	0	1	1	0	1	1	0	0	1	0	1
DAA_{DNA-CG}	0	1	0	1	0	1	0	1	0	1	0	1
DAD_{DNA-CG}	0	1	1	1	0	1	1	0	1	0	0	0
ADD_{DNA-CG}	1	0	0	0	0	0	0	0	0	0	0	0
ADA_{DNA-CG}	1	0	1	1	0	1	1	0	1	1	0	0
AAD_{DNA-CG}	1	1	0	1	0	0	1	0	0	0	0	0
AAA_{DNA-CG}	1	1	1	1	0	1	0	0	0	0	0	0

state	logic gate							
	none	none	none	Toffoli	none	none	none	none
$distance d(N_4....O_6) = 2.835 \text{ \AA}.$	none	none	none	Toffoli	none	none	none	none

* $distance d(N_4....O_6) = 2.835 \text{ \AA}.$

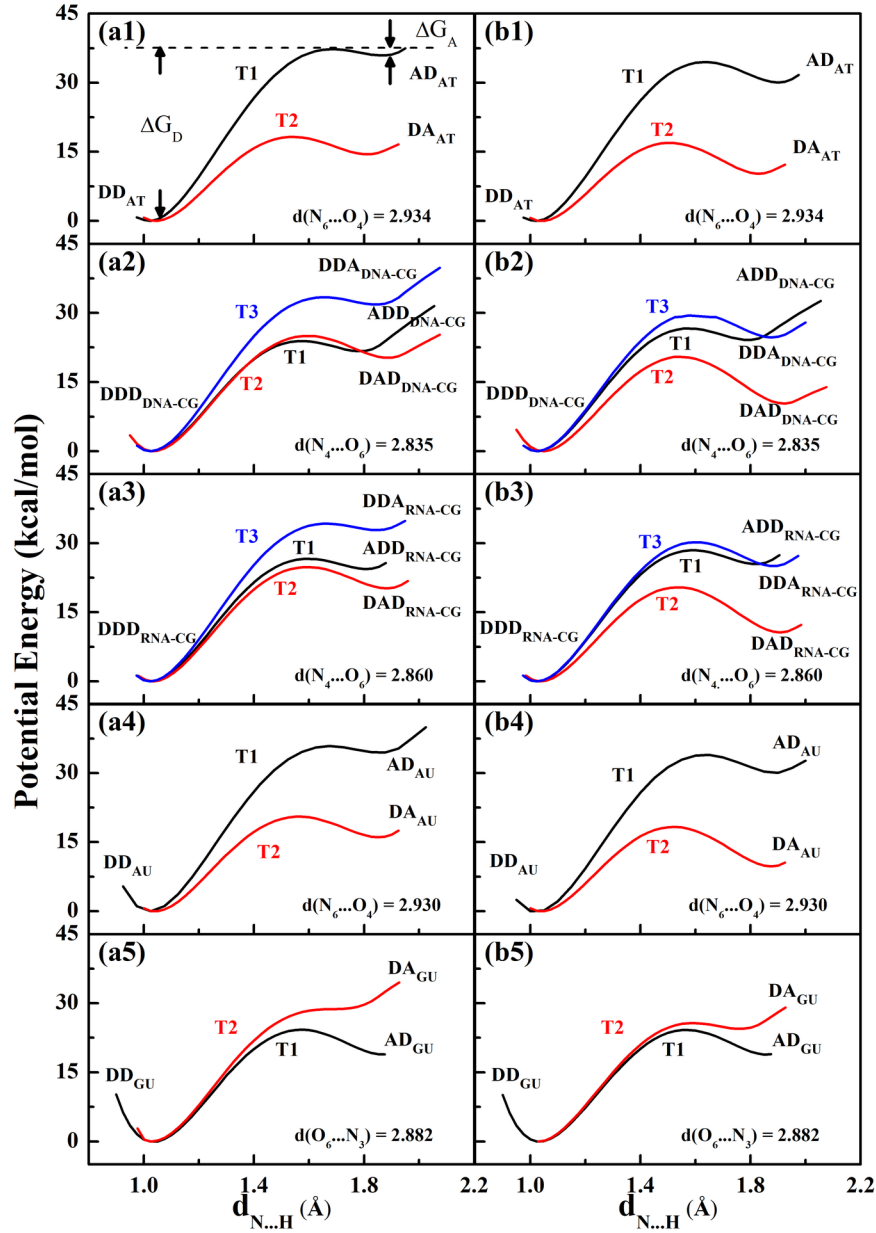


Figure S1: Potential energy of proton transfer. The systems are (a) in vacuum and (b) in the aqueous system; the nucleotide base pairs are (1) DNA: A=T, (2) DNA: C≡G, (3) RNA : C≡G, (4) RNA: A=U, and (5) RNA: G=U. T1, T2, and T3 indicate the transfer process for protons H₁, H₂, and H₃, respectively. All proton transfer potential surfaces contain an asymmetric double-well. ΔG_D (ΔG_A) is the barrier height from the donor state (the acceptor state) to the barrier top and it is much larger than the thermal energy $k_B T$ at room temperature. When the residue pairs are in aqueous solution, it is explicitly shown that ΔG_D (ΔG_A) is increased. Under such high energy barriers, there is a distinct separation between the donor state and the acceptor state, where the donor (acceptor) state can be defined as either |0⟩ (|1⟩) or |1⟩ (|0⟩). In Appendix, Eq.(A3) shows the superposition of the two states |0⟩ and |1⟩, and then the qubit state can be obtained.

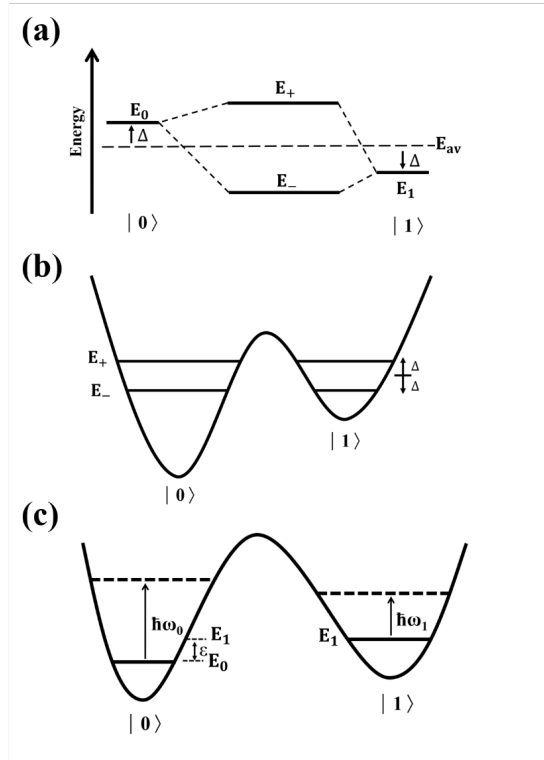


Figure S2: Energy level diagram and asymmetric double-well system. (a) The energy level diagram for the two-level system in vacuum. (b) An asymmetric double-well system with two eigenenergies E_- and E_+ of the molecular orbital in vacuum. The double-well local minima are labeled as $|0\rangle$ and $|1\rangle$. (c) An asymmetric double-well system for the spin-boson model in solution. The two states $|0\rangle$ and $|1\rangle$ are described by the spin Hamiltonian and the solvent degrees of freedom is depicted by the boson Hamiltonian. The energies E_0 and E_1 correspond to the ground states of the two-well state, $|0\rangle$ and $|1\rangle$, respectively.

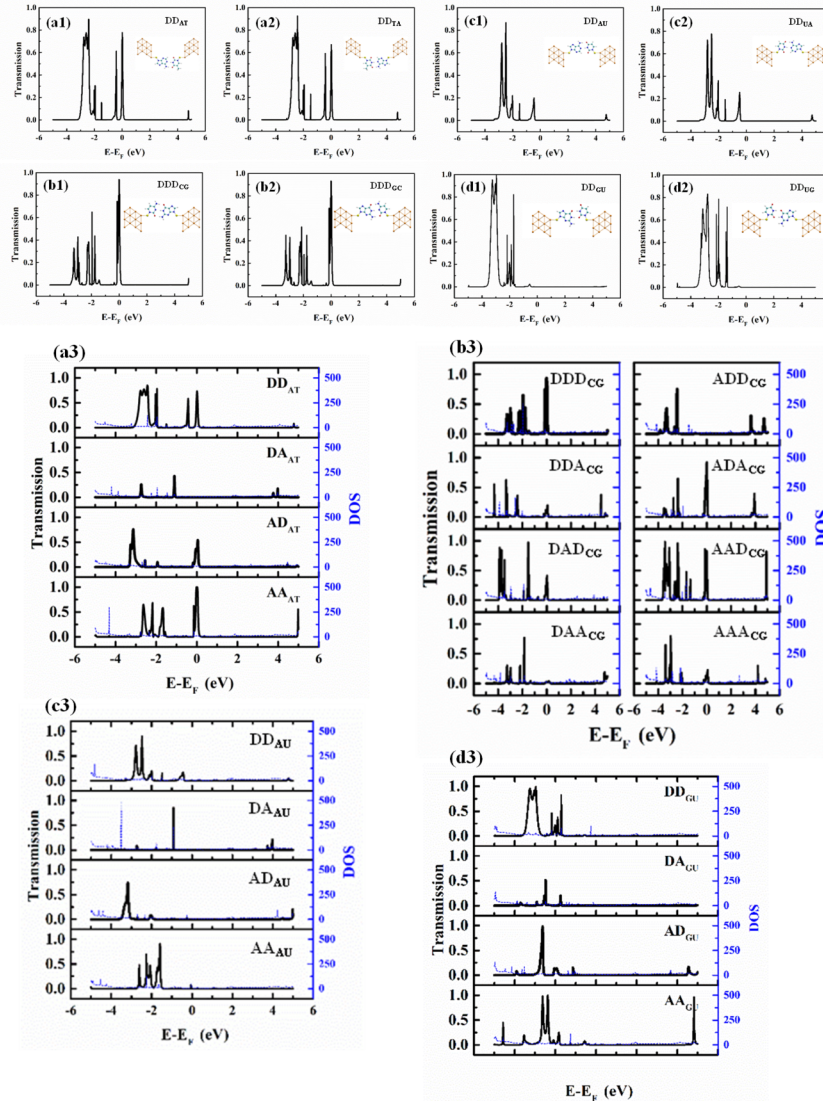


Figure S3: TS (left, in black) and DOS (right, in blue) of the nucleobase pairs. (a1-a3) AT, (b1-b3) CG, (c1-c3) AU, and (d1-d3) GU. The truth tables are summarized in Table 1.

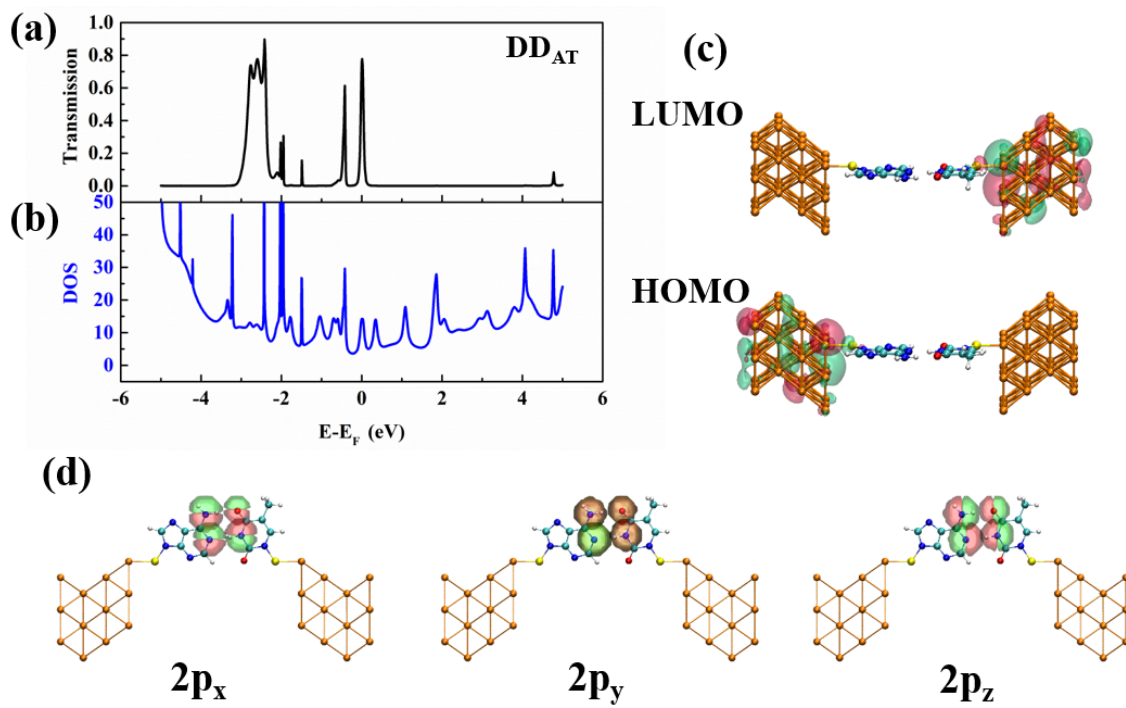


Figure S4: TS and DOS for the AT nucleobase pair. (a) TS, (b) DOS, (c) molecular orbital (MO) analysis for HOMO and LUMO, where the charge separation is clearly shown between HOMO and LUMO, (d) atomic orbital (AO) analysis. The 2p_x, 2p_y, and 2p_z orbitals are shown for the N-atom and O-atom. It clearly shows the overlap of the 2p_y orbitals.

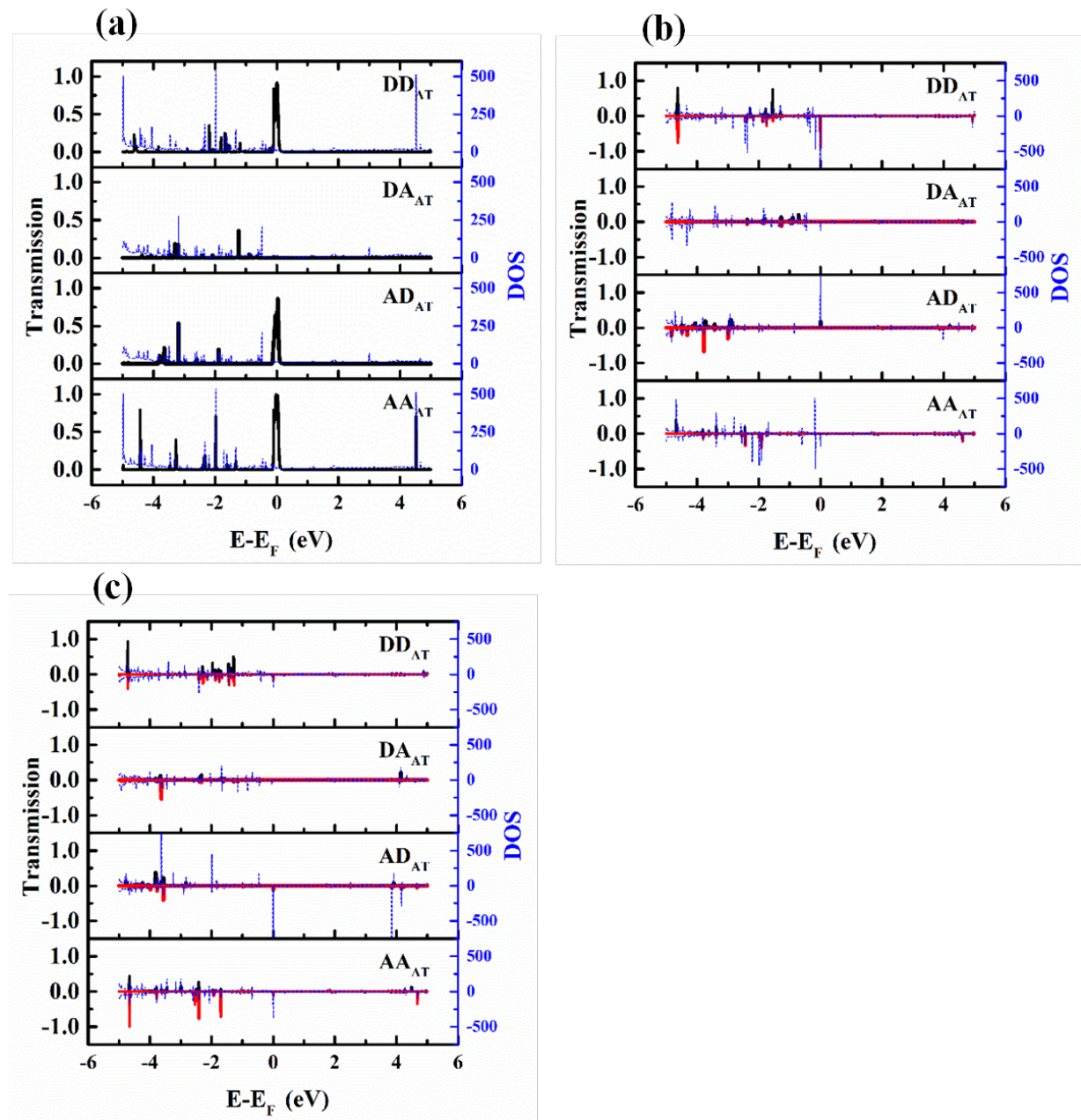


Figure S5: Spin effect on TS (left, in black) and DOS (right, in blue) of the nucleotide AT base pairs at the (L-phosphate, R-phosphate) charge (-1, 1). The spin state is (a) the singlet, (b) the triplet and (c) the quintet in which the spin up (down) is colored black (red). The truth tables are summarized in Table 2.

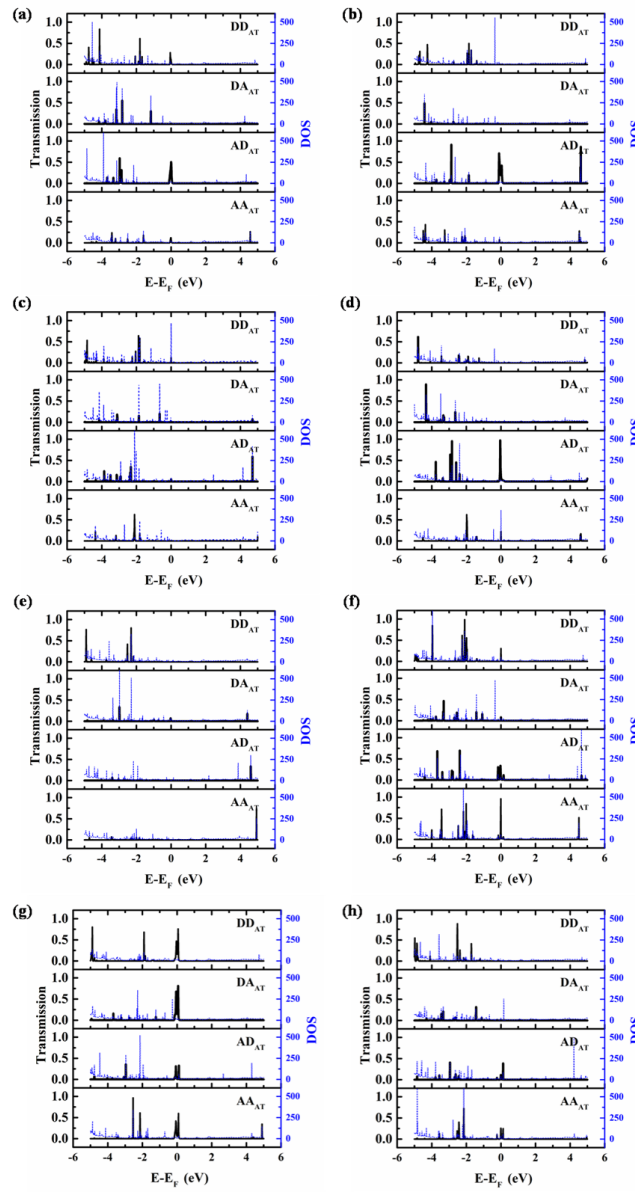


Figure S6: Charge effect on TS (left, in black) and the DOS (right, in blue) of the AT nucleotide base pair. The (L-phosphate, R-phosphate) charges are (a) (0, 0), (b) (0, -1), (c) (-1, 0), (d) (0, -2), (e) (-2, 0), (f) (-1, -2), (g) (-2, -1) and (h) (-2, -2). The truth tables are summarized in Table 3.

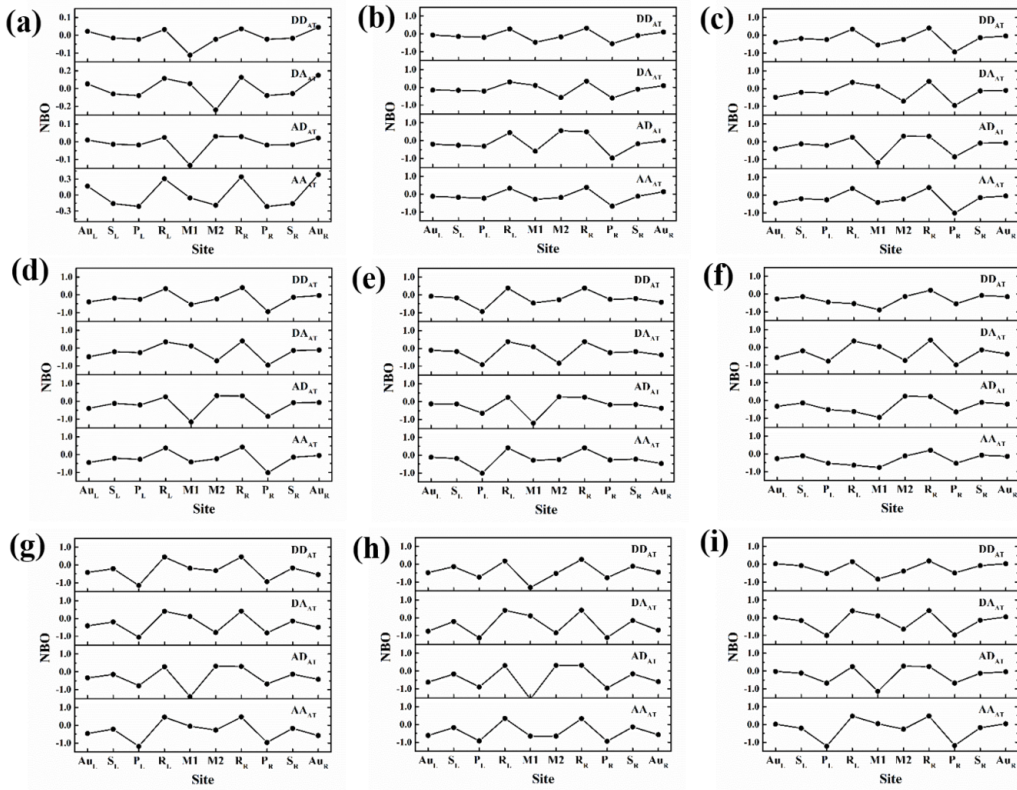


Figure S7: NBO charge distribution of the nucleotide AT base pair. The (L-phosphate, R-phosphate) charges are (a) (0, 0), (b) (0, -1), (c) (-1, 0), (d) (0, -2), (e) (-2, 0), (f) (-1, -2), (g) (-2, -1), (h) (-2, -2) and (i) (-1, -1). The regions are divided into the Au_{L(R)} electrode, the interfacial S_{L(R)} atom, the phosphate P_{L(R)} group, the ribose R_{L(R)} group, and the L(R)-nucleobase M1(2) group, where the subscript L(R) denotes the left (L) and right (R) sides of the AT base pair.

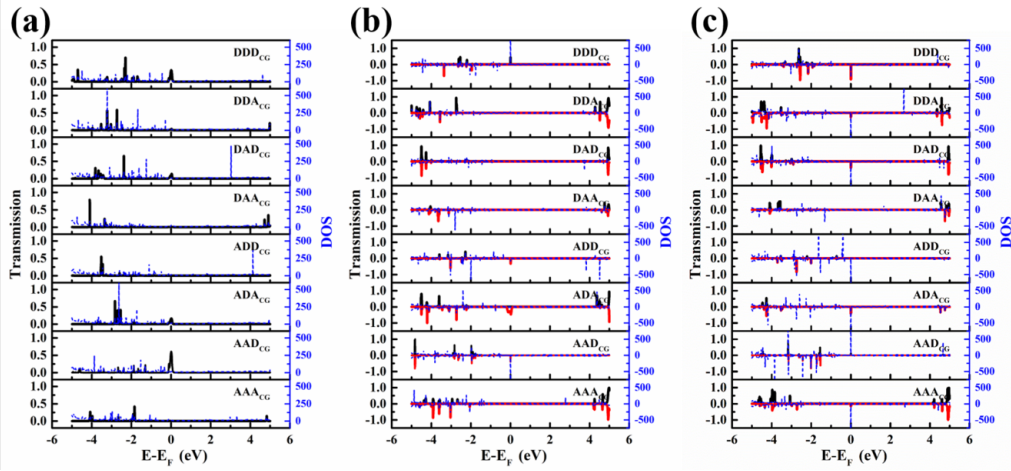


Figure S8: Spin effect on TS (left, in black) and the DOS (right, in blue) of the DNA-CG nucleotide base pairs at the (L-phosphate, R-phosphate) charges (-1, 1). The spin state is (a) the singlet, (b) the triplet and (c) the quintet in which the spin up (down) is colored black (red). The truth tables are summarized in Table S3.

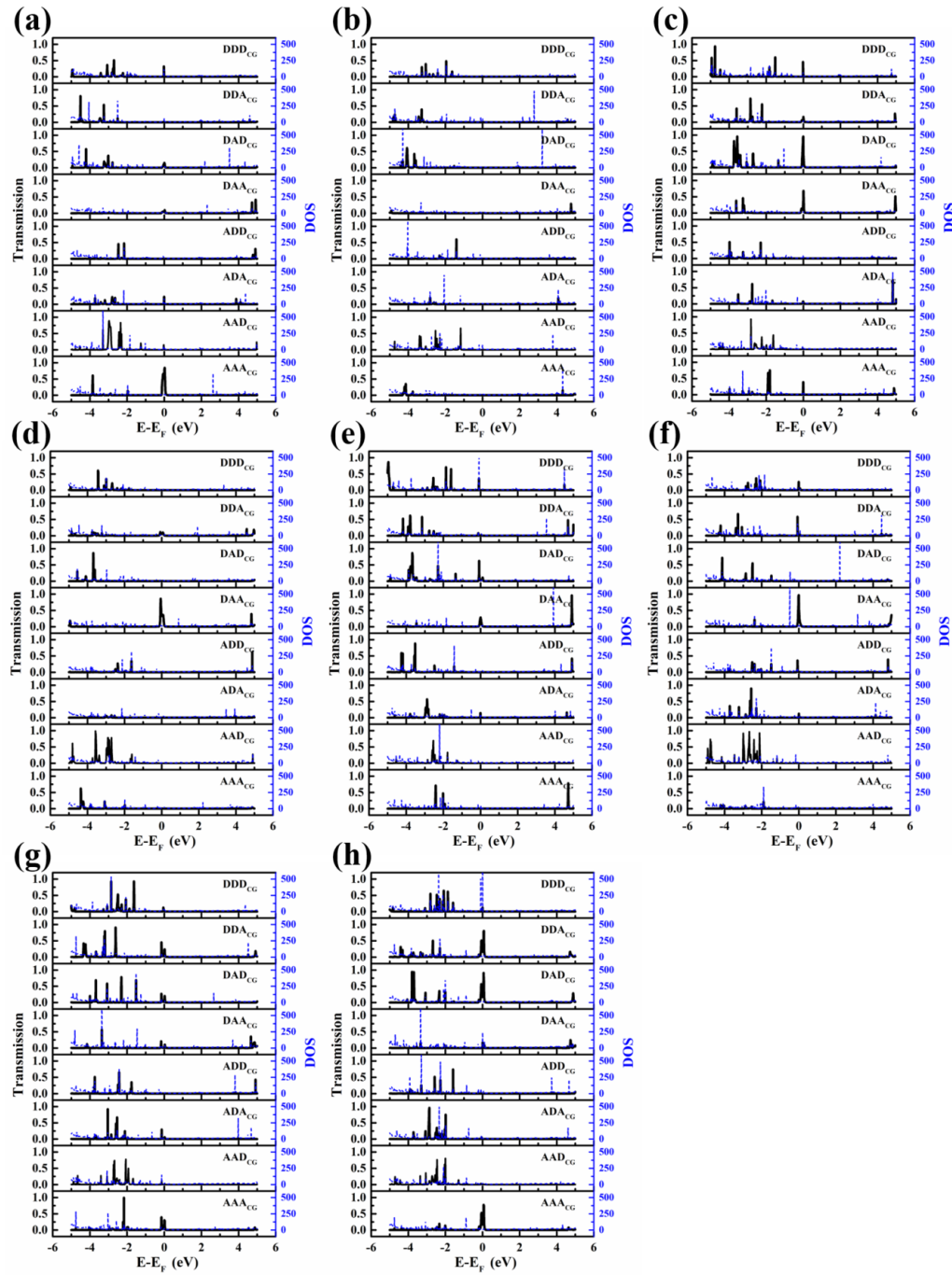


Figure S9: Charge effect on TS (left, in black) and the DOS (right, in blue) of the DNA-CG nucleotide base pairs. The (L-phosphate, R-phosphate) charges are (a) (0, 0), (b) (0, -1), (c) (-1, 0), (d) (0, -2), (e) (-2, 0), (f) (-1, -2), (g) (-2, -1) and (h) (-2, -2). The truth tables are summarized in Table S4.

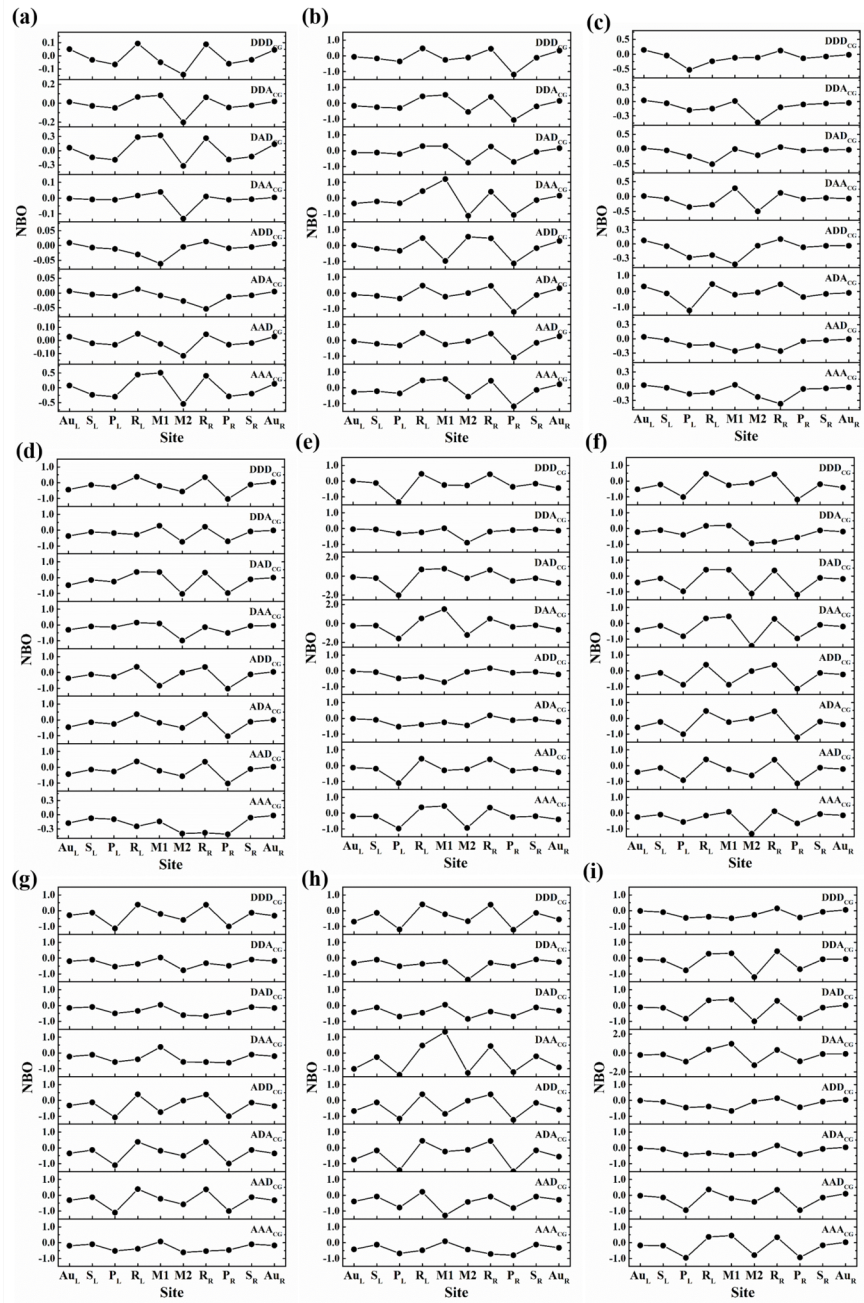


Figure S10: NBO charge distribution of the DNA-CG nucleotide base pair. The (L-phosphate, R-phosphate) charges are (a) (0, 0), (b) (0, -1), (c) (-1, 0), (d) (0, -2), (e) (-2, 0), (f) (-1, -2), (g) (-2, -1), (h) (-2, -2) and (i) (-1, -1). The regions are divided into the Au_{L(R)} electrode, the interfacial S_{L(R)} atom, the phosphate P_{L(R)} group, the deoxyribose R_{L(R)} group, and the L(R)-nucleobase M1(2) group, where the subscript L(R) denotes the left (L) and right (R) sides of the DNA-CG base pair.

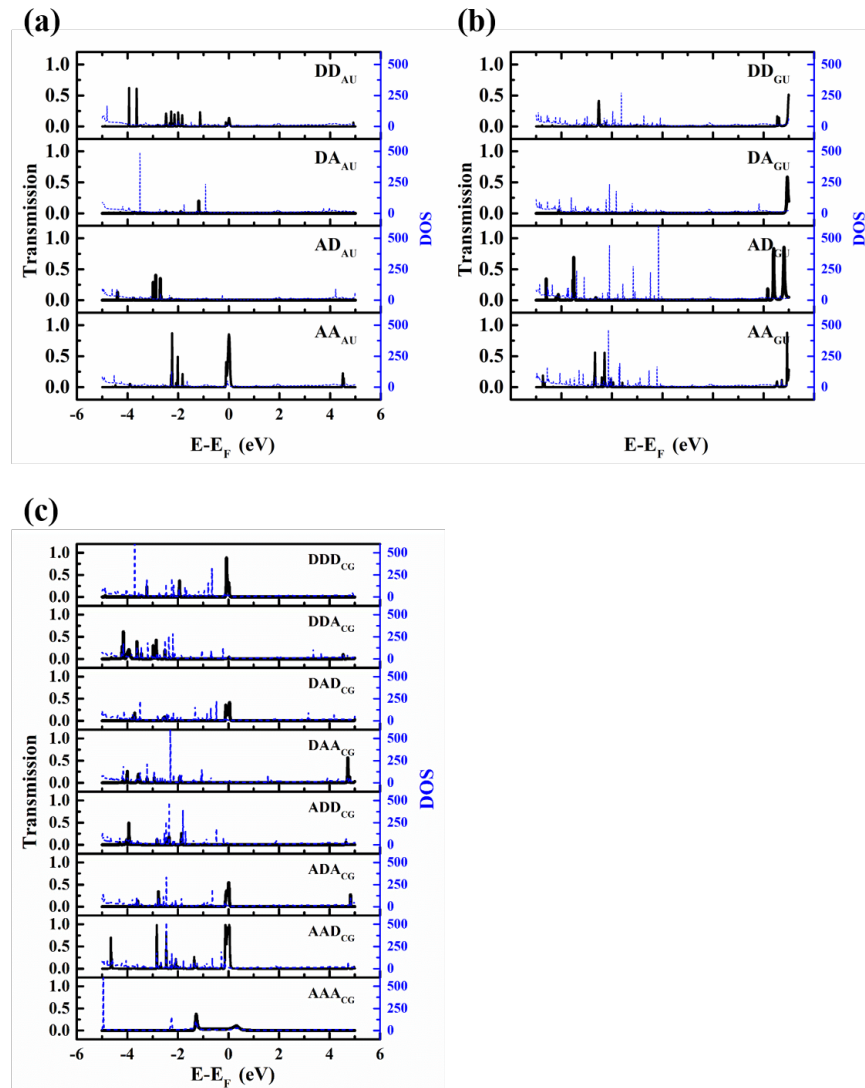


Figure S11: TS (left, in black) and DOS (right, in blue) of the RNA nucleotide base pairs. (a) AU, (b) GU and (c) RNA-CG. The spin state is the singlet state, and the (L-phosphate, R-phosphate) charges are (-1, -1). For GU base pairs, there is no $TS(D_e)$ peak and no qubit states.

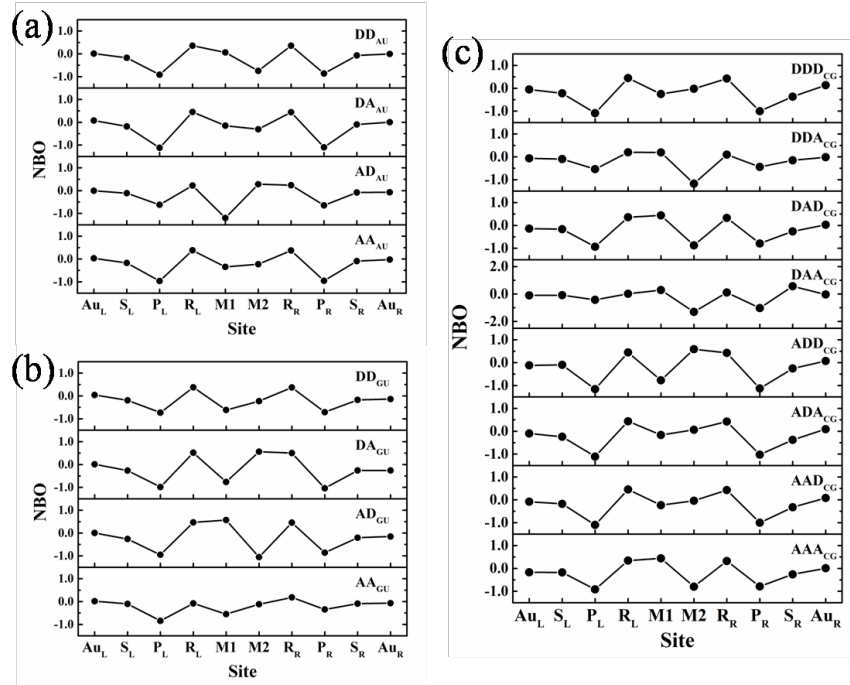


Figure S12: NBO distribution of the RNA nucleotide base pairs. (a) AU, (b) GU and (c) RNA-CG. The spin state is the singlet state, and the (L-phosphate, R-phosphate) charges are (-1, -1).

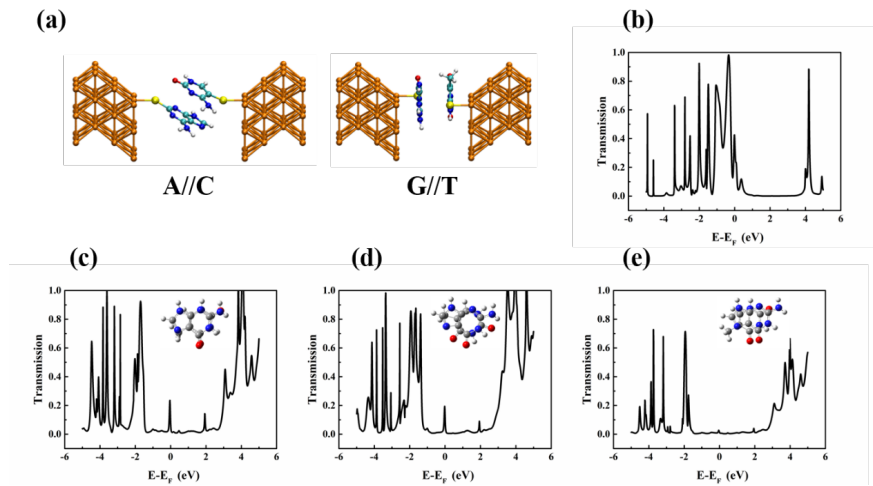


Figure S13: The molecular junctions and TS along the same strand. (a) The parallel stacked AC nucleobases and stacked GT nucleobases. TS of (b) the eclipsed AC nucleobases, (c) the eclipsed GT nucleobases, (d) the staggered GT nucleobases, and (e) the shifted GT nucleobases.

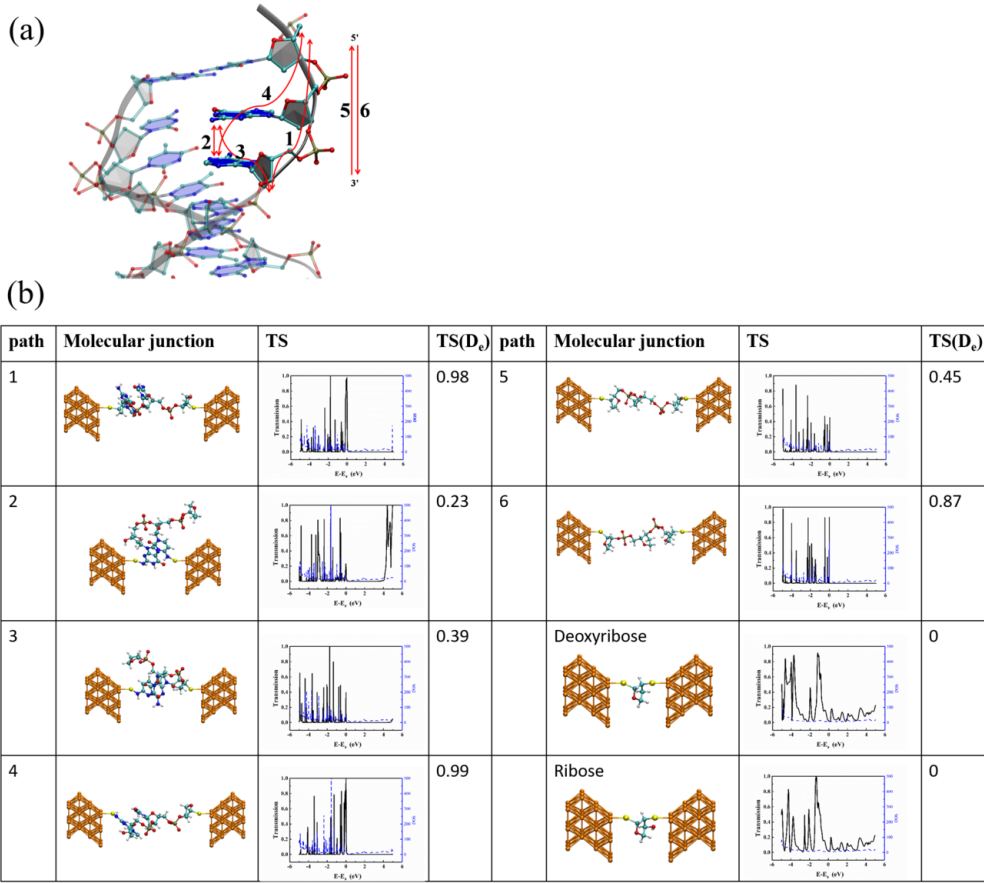


Figure S14: Molecular junctions and TS of DNA. (a) Electron transfer pathway in DNA. There are 6 possible pathways. (b) Molecular junctions and TS for paths in (a). The conductance of each deoxyribose and ribose group is zero; however, when it is combined with the phosphate group, it can conduct electrons.

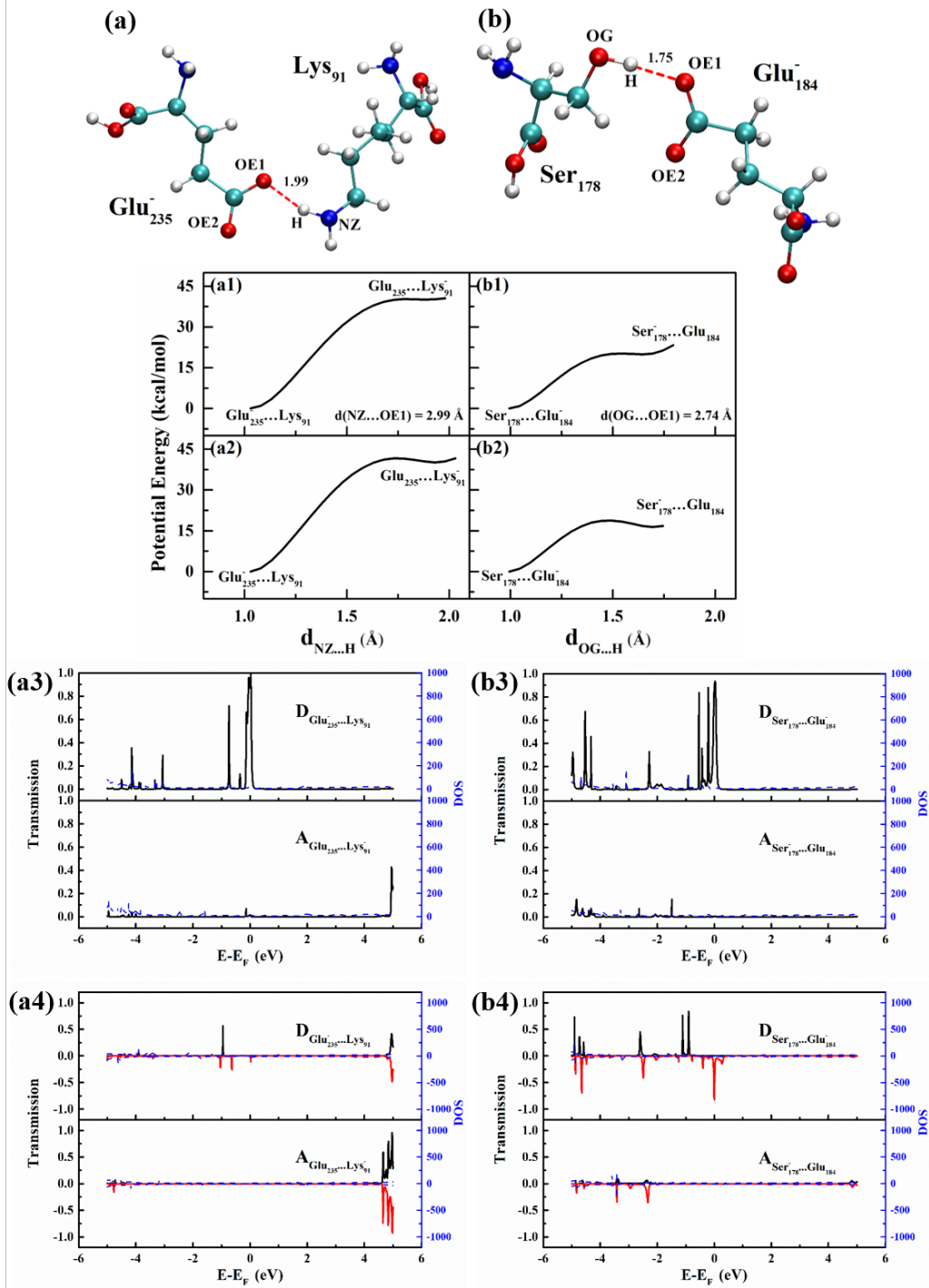


Figure S15: PCET of the amino acid pair: (a) $\text{Glu}_{235}^- \cdots \text{Lys}_{91}$ structure and (b) $\text{Ser}_{178} \cdots \text{Glu}_{184}^-$ structure. The proton transfer potential energy surface is (a1 and b1) in vacuum and (a2 and b2) in aqueous solution, TS of (a3 and b3) the singlet state and (a4 and b4) the triplet state in which the spin up (down) is colored by black (red).

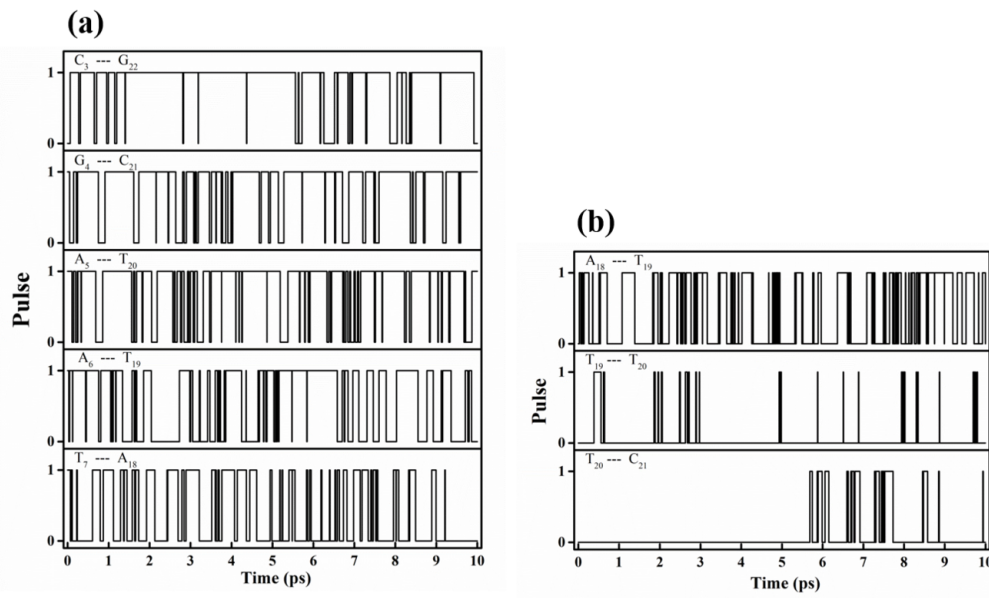


Figure S16: Pulse signal vs MD time. (a) Pulse outputs of the H-bond distance changes in the nucleotide base pairs C₃—G₂₂, G₄—C₂₁, A₅—T₂₀, A₆—T₁₉ and T₇—A₁₈. (b) Pulse outputs of the distance between the stacked nucleobases A₁₈—T₁₉, T₁₉—T₂₀ and T₂₀—C₂₁. Each nucleic acid sequence shows a distinct signal pattern.